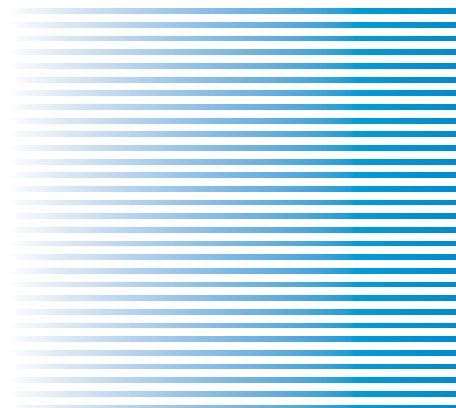
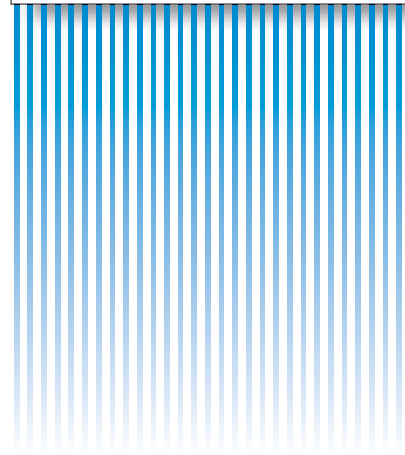
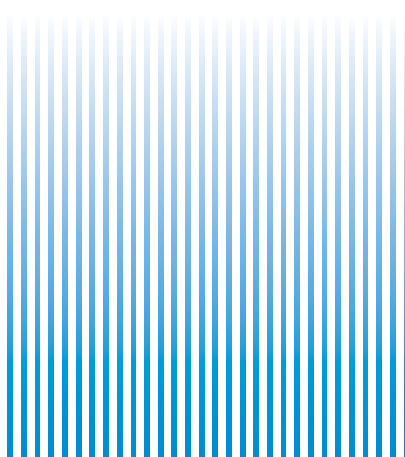
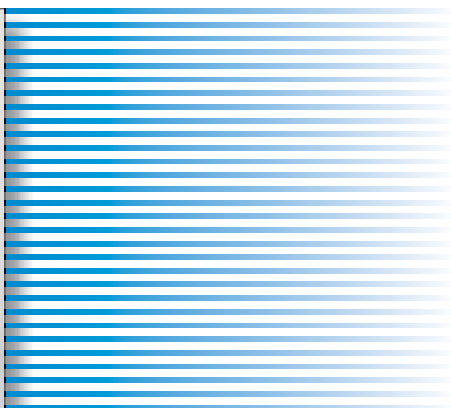


# ADVANCE

Heat Pump with Natural Refrigerants



**Cover Story**

The photo in the upper left position on the cover shows the CO<sub>2</sub> refrigerant rotary compressor which is provided in ECO CUTE. The photo in the upper right shows the heat transfer pipe of the twist & spiral gas cooler which serves as a heat exchanger between the refrigerant and water. The photo in the center shows the CO<sub>2</sub> refrigerant heat pump hot water system, "ECO CUTE". The photo in the lower left shows the heat exchanger employing micro-channels. The photo in the lower right shows the commercial CO<sub>2</sub> refrigerant heat pump hot water system.

- **Editorial-Chief**

*Ryuichi Yamaguchi*

- **Editorial Advisors**

*Chisato Kobayashi*

*Yasuyuki Sano*

*Makoto Egashira*

*Junichi Kitsuki*

*Hiroaki Kawachi*

*Masayuki Masuda*

*Satoshi Itoda*

*Kiyoji Kawai*

*Kazuhiisa Hemmi*

*Taizo Kittaka*

*Hidenori Takita*

*Itsuo Seki*

*Katsuhiko Hase*

*Kazumasa Mitsunaga*

- **Vol. 120 Feature Articles Editor**

*Satoru Kotoh*

- **Editorial Inquiries**

*Makoto Egashira*

Corporate Total Productivity Management  
& Environmental Programs

Fax +81-3-3218-2465

- **Product Inquiries**

Strategic R&D Planning Department

Advanced Technology R&D Center

Fax +81-6-6497-7285

**Mitsubishi Electric Advance** is published on line quarterly (in March, June, September, and December) by Mitsubishi Electric Corporation.  
Copyright © 2007 by Mitsubishi Electric Corporation; all rights reserved.  
Printed in Japan.

**CONTENTS****Technical Reports**

Overview .....	1
by <i>Fumiaki Baba</i>	
The Current Status of and Future Trends in Heat Pump Technologies with Natural Refrigerants .....	2
by <i>Naoki Tanaka</i> and <i>Satoru Kotoh</i>	
Development of CO <sub>2</sub> Heat Pump Hot Water System "ECO CUTE" .....	6
by <i>Tetsuji Okada</i>	
Rotary Compressor for a CO <sub>2</sub> Heat Pump Water Heater .....	9
by <i>Hideaki Maeyama</i> and <i>Shinichi Takahashi</i>	
Wear-Reducing Technologies for Rotary Compressors Using CO <sub>2</sub> Refrigerant .....	13
by <i>Hideto Nakao</i> and <i>Naotaka Hattori</i>	
Performance Analysis of Scroll Compressors Using CO <sub>2</sub> Refrigerant .....	17
by <i>Mihoko Shimoji</i> and <i>Toshiyuki Nakamura</i>	
Prototype and Performance Evaluation of Refrigerant-Refrigerant Microchannel Heat Exchanger .....	20
by <i>Susumu Yoshimura</i> and <i>Shinichi Wakamoto</i>	

# Overview



Author: *Fumiaki Baba\**

The Kyoto Protocol, which came into effect in 2005, requires all industrialized nations to reduce global greenhouse gas emissions by 5% from 1990 levels during the period from 2008 to 2012. Accordingly, countries have worked hard to develop and introduce technologies for reducing such emissions and meeting their respective targets, for example, -6% for Japan. Heat pump technologies applied to air-conditioning equipment, refrigerators, and water heaters feature high energy efficiencies and effectively reduce greenhouse gas emissions. In particular, the coefficient of ozone destruction of carbon dioxide gas (CO<sub>2</sub>), which abounds in nature, is zero and the gas is neither inflammable nor toxic. By using this environment-friendly carbon dioxide as a refrigerant gas for heat pumps, we can create environment-friendly systems.

In order to use carbon dioxide as a refrigerant, the operating pressure needs to be three to five times that of the conventional refrigerant, which is equivalent to approx. 100 atmospheres. Carbon dioxide under such high pressure exhibits a supercritical state in which carbon dioxide has both gaseous characteristics (diffusivity) and liquid characteristics (solubility). In a supercritical state, the density typically fluctuates largely. Therefore, it is important to carefully consider ways to reduce leakage loss and friction loss in the compressor, a pressure-proof design and the path-pattern design of the refrigerant heat exchanger in order to use carbon dioxide in heat pump equipment. In addition, heat pump equipment using carbon dioxide refrigerant can supply hot water at 90°C, which is difficult with the conventional refrigerant. The technology thus has a wide range of applications. Conventional heat pump systems used to have the weakness that their performance decreased in cold conditions. However, recently developed systems with high energy efficiencies can maintain high performance even in cold conditions, with the result that heat pump equipment is increasingly being used in cold regions.

This issue introduces the latest heat pump systems using carbon dioxide natural refrigerant and development of the elements of heat pump systems, such as compressors and refrigerant heat exchangers. Mitsubishi is committed to continuing to develop high-performance energy-saving systems to help curb global warming.

# *The Current Status of and Future Trends in Heat Pump Technologies with Natural Refrigerants*

Authors: Naoki Tanaka\* and Satoru Kotoh\*\*

## 1. Introduction

There is currently an urgent need to develop technologies for the use of environmentally-friendly refrigerants that are low in global warming potential (GWP). Mitsubishi has already developed and commercialized refrigerators and heat pump water heaters that use environmentally-friendly natural refrigerants. We are persisting with R&D efforts aimed at commercialization of next-generation heat pump systems that use natural refrigerants. The following paragraphs introduce the current status and future aspects of Mitsubishi's technological development.

## 2. Trends in the Regulation of Refrigerants

The trends in the regulation of the use of HFC (Hydro Fluorocarbon) refrigerants currently used in air-conditioning systems, heat pump water heaters and refrigerators are described below.

### (1) Emission control of greenhouse gas after enforcement of the Kyoto Protocol

Conforming to the 1994 UN Framework Convention on Climate Change for the prevention of global warming, the Kyoto Protocol was adopted as a concrete measure to control greenhouse gas emissions (in 1997). Thereafter, with the ratification by Russia, the Kyoto Protocol was enforced in 2005. The relevant industrialized nations are required to reduce greenhouse gas emissions by 6% (down from 1990 levels) in Japan for example during the first commitment period (2008 to 2012). Flon's substitutes are designated as greenhouse gases to be reduced in accordance with the Protocol because they have a high GWP and their emissions are expected to be reduced by maximum efforts from the participating nations.

### (2) Outline of fluorinated gas regulations in Europe <sup>(1)</sup>

The target of the regulations is to confine or reduce the emissions of fluorinated warming gases, HFC, PFC (perfluorocarbon) and SF<sub>6</sub> (sulfur hexafluoride) which are targeted by the Kyoto Protocol. For purposes of confining fluorinated gases, some requirement items related to fixed-type refrigeration, air-conditioning and heat pumps became compulsory, effective July 4, 2007,

with respect to gases that have a global warming potential of 150 or higher.

## 3. Trends in Flon Elimination Technologies for Heat Pump Systems

### 3.1 Natural refrigerants as flon-free refrigerants

Fluorocarbon refrigerants currently used in heat pump systems with vapor compression refrigeration cycles are safe, highly efficient and can be used extensively. New heat pump system designs are making such refrigerants increasingly suitable for use.

The required characteristics of refrigerants a decade or so ago did not include requirements associated with global environmental conservation (such as protection of the ozone layer and prevention of global warming), although requirements against toxicity and flammability were specified. Today, with the prevention of global warming being a mandatory issue, materials with little or no influence on the global environment are required most, with the requirement of low toxicity or flammability being emphasized less than it was before.

Because the refrigerants currently being used are considered to have a considerable influence on global warming if emitted into the air, it is necessary to reuse or destroy them without atmospheric emission. However, as things stand, it is very difficult to meet these requirements.

The focus has gradually turned to natural refrigerants regarding global environmental preservation. At present, CO<sub>2</sub>, hydrocarbons (propane, propylene, etc.), ammonia, water, and air are considered as possible flon-free refrigerants. Of the potential candidates mentioned above, air is different from the others as applied to the vapor compression refrigeration cycle, however, it is included from a functional point of view. Although these natural refrigerants are excellent in terms of global environmental preservation, they possess shortcomings in chemical characteristics and/or thermo-physical properties, as shown in Table 1. We have to tackle such difficulties and find solutions, in terms of both hardware and software.

Table 1 Characteristics of natural refrigerants

Refrigerant		CO <sub>2</sub>	Hydrocarbon	Ammonia	Water	Air
Chemical properties	Toxicity/flammability	○	Δ	Δ	○	○
	Material deterioration	○	○	Δ	○	○
	Chemical stability	○	○	Δ	○	○
Thermophysical properties	Moderate boiling point	Δ	○	○	Δ/○**	Δ
	Capacity per unit volume	○	○	○	Δ/○**	○
	Theoretical COP	Δ/○*	○	○	○	Δ
	Moderate discharge temperature	○	○	○	○	○
Global environmental property	Ozone layer	○	○	○	○	○
	Warming	○	○	○	○	○

\* Evaluated with air-conditioners/water heaters.

\*\* Evaluated for source-of-heat temperature at low/high

○: Acceptable

Δ: Unacceptable (shadowed)

### 3.2 Targets of R&D

Looking at CO<sub>2</sub> and hydrocarbons in particular, special attention must be paid to the following two characteristics for their use as refrigerants in heat pump systems.

CO<sub>2</sub>: because it has a low boiling point, systems will have to be designed to endure service pressures of 100 to 150 atmospheres, as the refrigerant exceeds the critical point.

Hydrocarbons: because hydrocarbons are flammable, it is necessary to take measures to reduce in the amount of refrigerant, to prevent leakage, and to eliminate the sources of ignition for the elimination of accidents when handling the material for repair and disposal after use.

Apparatuses that use these refrigerants have already been marketed. The target of R&D activities in this sense is to improve the performance of existing apparatuses or to expand the application field by developing new types of apparatuses.

## 4. Development of Flon-free Heat Pump Systems

The following descriptions refer to an outline of R&D activities aimed at developing flon-free heat pump systems that are underway as part of the NEDO (New Energy and Industrial Technology Development Organization) project and the challenges and present circumstances related to major element devices incorporated in heat pump systems.

### 4.1 Participation in the NEDO development project for next-generation, flon-free apparatuses

Mitsubishi has participated in the two NEDO projects described below to promote the basic technological development of next-generation, flon-free apparatuses.

(1) Double-stage compressor heat pump water heaters

for cold district

We conducted an R&D program (FY2005 to FY2006) under the theme of “double-stage compressor heat pump water heaters using CO<sub>2</sub> refrigerant for cold district” in compliance with the target of “improvement in efficiency and down-sizing of high-efficiency water heaters” of the Strategic Development of Energy Conservation Technology Project.

The ratio of suction pressure (low pressure) of the compressor to the discharge pressure (high pressure) is large and subjects the compressor to harsh operating conditions in cold district where the lowest temperatures range from -10 to -20°C, which theoretically lowers both the water-heating capacity and the coefficient of performance (COP). For this reason, this R&D focused on the improvement of the water heating capacity and COP. The performance and reliability were to be improved by a mechanism that includes the compression stroke divided into two stages and the refrigerant injection at intermediate pressure. In addition, improvement in the thermal insulation performance of the hot-water tank and development of a high-efficiency gas cooler (heat exchanger) were also included in R&D activities for a higher COP.<sup>(2)</sup>

(2) Multi-air conditioners for buildings

We have also been developing multi-air conditioners for buildings using a CO<sub>2</sub> refrigerant as part of the development of Non-fluorinated Energy-Saving Refrigeration and Air Conditioning Systems for Business Use under the “Development of Non-fluorinated Energy-Saving Refrigeration and Air Conditioning Systems (FY2005 to FY2007)”.

This development program is characterized by aiming at high performance systems through the combination of a recovery function for cooling exhaust heat, an energy reutilization function with a power recovery expander and gas cooler radiation mechanism that

saves energy by making use of CO<sub>2</sub> characteristics. The development target is to achieve an annual operating efficiency equal to that of the current models, or higher.

Figure 1 shows the major component devices and their characteristics.

#### 4.2 Technological challenges of developing CFC-free refrigerant heat pump component devices

##### (1) Expansion power recovery circuit

One of the means of recovering expansion power is with an expander. An expander is driven by the expansion of high-pressure refrigerant. The resultant driving force is used for compression or other types of power. The most difficult challenge with this mechanism is to control the operating conditions, such as the rotating speed of the expander and the compressor, for maximum power recovery.

##### (2) Heat exchangers

###### 1) A gas cooler for water heaters

During heat exchange within the supercritical range, the temperature of CO<sub>2</sub>, which is incondensable, gradually lowers while passing heat to water, thus there is no range where the temperature remains constant. For this particular characteristic, a gas cooler for water heaters can affect ideal counter-current heat exchange with little temperature difference between the water and the refrigerant. Mitsubishi employed a twisted-tube gas cooler <sup>(2)</sup> in

which a CO<sub>2</sub>-flow pipe is wrapped around the slot in the twisted water piping. Mitsubishi will improve the pipe diameter, joining method, and insulation method for improved performance of the gas cooler.

###### 2) A gas cooler for air-conditioners

Most gas coolers for air-conditioners employ a single-direction heat exchange method for the air. It is difficult to use a complete counter-flow type method like that employed in water heaters. However, with a structure containing a number of microchannels laid out in parallel to provide counter-flow channels for heat exchange with the air, the efficiency of the gas cooler can be improved.

###### (3) Compressor

When using CO<sub>2</sub> as natural refrigerant, compared with the current HFC refrigerant, the discharge pressure of the compressor nearly triples to 10 MPa and the rate of discharge pressure to suction pressure almost triples. As a result, internal losses in the compressor such as leakage loss and mechanical loss increase. Naturally, it becomes necessary to improve the performance against loss and also reliability, by increasing the structural strength as well as wear/friction durability.

Mitsubishi has developed small-capacity rotary type compressors <sup>(3),(4),(5)</sup> for household heat pump water heaters. In addition, for large-capacity applications, the development of a CO<sub>2</sub> scroll compressor to be used in business-use heat pump water heaters or building-type multi-air conditioners is underway.

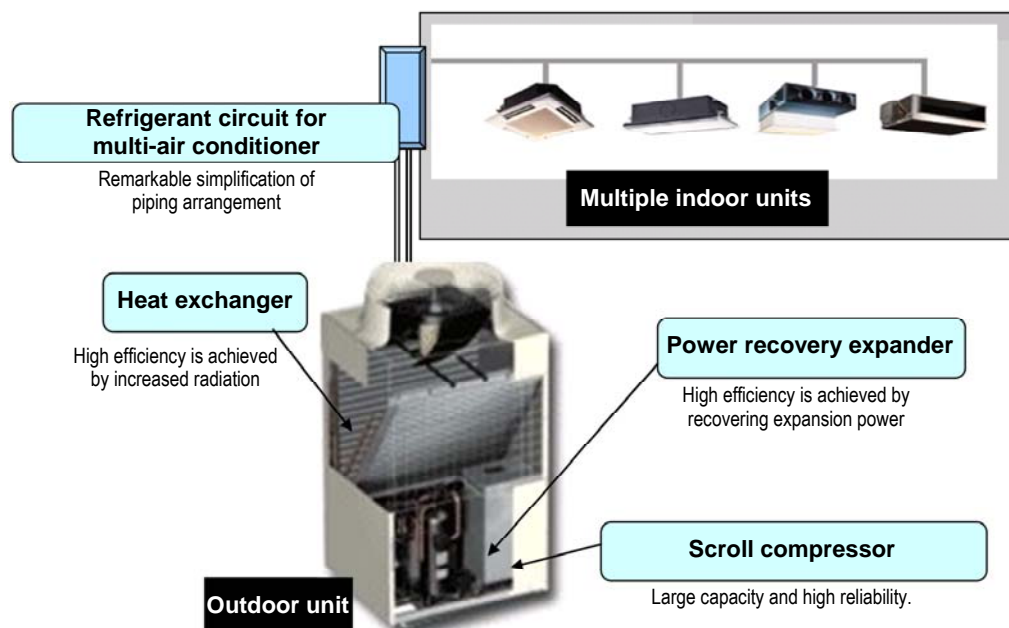


Fig. 1 Development points of a multi-air conditioner for buildings with CO<sub>2</sub> refrigerant

#### (4) Power recovery expander

Since the expansion enthalpy drop in CO<sub>2</sub> circuits is much larger than that of an HFC refrigerant, recovery and reuse of expansion power are effective, resulting in improved efficiency.

Power recovery expanders with the same basic structure as a compressor are being developed at present. To improve efficiency, special attention is being paid to the reduction of internal leakage loss and friction loss.

#### 5. Conclusion

This paper outlined Mitsubishi's current R&D activities related to technologies for natural refrigerant air-conditioners. Mitsubishi will improve the efficiency and reliability of products equipped with the technologies discussed above.

#### References:

- (1) DIRECTIVE 2006/40/EC OF THE EUROPEAN PARLIAMENT AND OF THE COUNCIL (2006).
- (2) T. Okada: CO<sub>2</sub> Refrigerant Heat Pump Water Heater "ECO CUTE", Mitsubishi Technical Report, 81, No.3, pp. 185-188, 2007.
- (3) H. Maeyama et al.: "Development of a Compressor for CO<sub>2</sub> Heat Pump with a Single Rotary Mechanism," International Compressor Engineering Conference at Purdue (2006), C056.
- (4) H. Maeyama: Development of a Compressor for CO<sub>2</sub> Heat Pump Water Heater with a Single Rotary Mechanism, The International Symposium on New Refrigerants and Environmental Technology 2006, pp. 217-222.
- (5) H. Maeyama: Rotary Compressor for CO<sub>2</sub> Heat Pump Water Heaters, Mitsubishi Technical Report, 81, No. 3, pp. 189-192, 2007.

# Development of CO<sub>2</sub> Heat Pump Hot Water System “ECO CUTE”

Author: Tetsuji Okada\*

## 1. Introduction

The market of CO<sub>2</sub> heat pump hot water system “ECO CUTE”, which complies with the Ministry of Economy, Trade and Industry’s CO<sub>2</sub> emission reduction plan, has been spreading rapidly. The new system launched in June 2006 employs Mitsubishi’s latest technologies and has been a commercial success thanks to its competitiveness. This report introduces the technologies of the compressor, heat exchanger, heat insulating material, etc. in the new system.

## 2. Environment of Electric Hot Water System Business

In March 2002, the “Outline for Promotion Effects to Prevent Global Warming” was established and specific countermeasures against global warming to be taken by various sectors were publicly announced by the government. Since the Kyoto Protocol came into effect in February 2005, the importance of countermeasures against global warming has grown to encompass all sectors and organizations in Japan related with energy and the environment, with the numerical targets specified for compliance.

The final energy consumed by the consumer and general household sector has increased largely, following the freight and passenger transport sector, so urgent countermeasures in these sectors are necessary. The outline mentioned above includes specific, detailed descriptions of countermeasures for the consumer sector, such as “expanding the range of application of top-runner standards”. From the trends of energy consumption by application, about 60% of energy is consumed by room heating and water heating systems in this sector.

The ratio of all-electric homes has been increasing year by year due to heavy marketing to the residential sector by electric power companies throughout the country. As a result, electric water heaters, IH cooking heaters, solar power generation systems, and the like are increasingly accepted in electricity markets. These groups of products are a key part of our all-electric strategy.

The Ministry of Economy, Trade and Industry has set a specific target of 5.2 million heat pump water heaters installed by FY2010. Both manufacturers and power companies have drawn up plans with their re-

spective policies and schemes. In addition, local governments are increasingly accepting applications by end users for grants or have established their own subsidy systems.

In this report, we discuss the technological features of the ECO CUTE heat pump water heater using environment-friendly CO<sub>2</sub> natural refrigerant (called HP water heater hereafter).

## 3. Features of ECO CUTE

ECO CUTE is a nickname commonly used by power companies and water heater manufacturers for HP electric water heaters that use natural refrigerant and are widely used in industry. Mitsubishi started to commercialize HP water heaters in FY2001, and a total of 100,000 units were actually sold from FY2001 to FY2005.

The technological features of Mitsubishi’s HP water heaters are as follows.

- (1) High-efficient heat pump system  
The performance is about 3 to 4 times that of conventional heaters.
- (2) Use of environment-friendly natural refrigerant  
CO<sub>2</sub> refrigerant, which does not destroy the ozone layer and has low global warming potential, is used.
- (3) Economical nighttime power is used.

## 4. Technological Features of Mitsubishi Products

Mitsubishi “diahot” has the largest share of the HP water heater market. In June 2006, we integrated the technologies of the “diahot” hot water tank with heat pump technologies used in our industry-leading air-conditioning systems, and launched new products as shown in Fig. 1 which are far superior to those of other manufacturers. The technological features of the products are described below.

- (1) High-efficiency compressor and high-efficiency heat exchanger were developed to achieve the industry-leading rating of COP4.9.
- (2) New foam insulation having 15% better insulating performance than conventional insulation material is used in the hot water tank, increasing the heat insulation capacity.



Fig. 1 Appearance of heat pump water heater ECO CUTE

#### 4.1 High-efficiency rotary compressor

The heat pump unit serving as the heat source of the water heater uses a rotary compressor whose performance has been proved in Mitsubishi air-conditioners. The HP water heater is a high-pressure shell type rotary system using a Poki Poki Motor for the first time in the industry; its performance and quality ensure sufficient reliability of the HP water heater. The key technologies of the compressor are as follows.

- (1) Use of high-efficiency Poki Poki Motor  
Mitsubishi's original Poki Poki Motor, with its high coil density and high efficiency, is used in the compressor of this water heater. Figure 2 shows the stator of the motor.

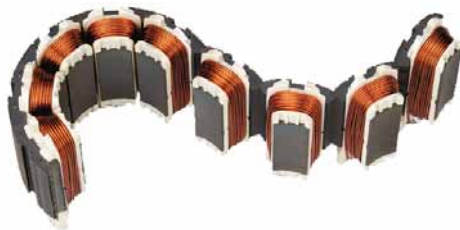


Fig.2 Appearance of Poki Poki Motor

The stator core of the Poki Poki Motor is open for coil winding, so the winding process is not spatially constrained and dead space is minimized. With a 20% higher line volume ratio (the space density of the copper coil) than conventional motors, the motor efficiency is 2% higher.

- (2) Use of wear-resistant vanes <sup>(2)</sup>  
Since CO<sub>2</sub> refrigerant requires a very high operating pressure (11.3 MPa), the reliability of sliding parts was expected to be vulnerable, so we coated the surface of sliding parts with super-hard DLC-Si (DLC containing silicone), thus improving reliability. The conventional nitrided vanes (for

air-conditioners) indicated low wear resistance when CO<sub>2</sub> refrigerant was used and failed to satisfy the required service life, so we more than doubled the load bearing characteristic and verified that the service life was sufficient.

#### 4.2 High-efficiency water-to-refrigerant heat exchanger

In addition to the compressor, this water heater system features Mitsubishi's new technology for heat exchangers. In the water-to-refrigerant heat exchanger (also referred to as gas cooler in water heaters) which heats water for hot-water supply to users, we used a newly developed "twist & spiral gas cooler". As shown in Fig. 3, the heat exchanger uses a twisted pipe with three lines of spiral grooves for a water pipe, which are prepared by a twisting method. A refrigerant pipe (thin pipe) is wound around the twisted pipe and connected to each other by zinc-free soldering for heat conduction. This arrangement increases the contact surfaces on both pipes, thus increasing the heat transfer area. The continuous spiral grooves in the twisted pipe accelerate the turbulence effect in the water and also help reduce pressure loss in the heat exchanger. Furthermore, three pipes are wound around the three spiral grooves in parallel to reduce the pressure loss in the refrigerant.

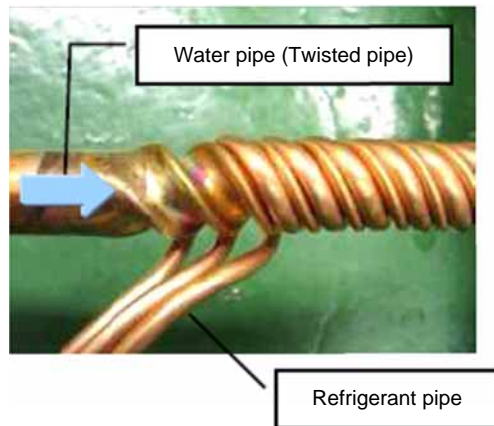


Fig. 3 Appearance of water-to-refrigerant heat exchanger

Since pressure loss is minimum in both the water pipe and refrigerant pipe, the efficiency of the compressor and heat transfer efficiency are improved, and the input to the circulation pump can be reduced.

The features of the heat exchanger are described below.

Figure 4 compares the heat transfer efficiency between Mitsubishi's twisted-pipe type heat exchanger and other types of heat exchangers. The figure clearly indicates that the twisted-pipe type has a far higher (more than double) heat transfer efficiency.

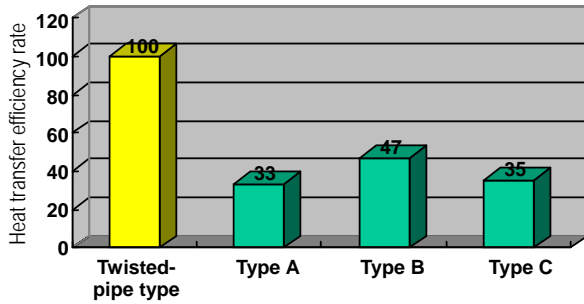


Fig. 4 Heat transfer efficiency per unit length of water pipe

### 4.3 Improvement of heat insulation of tank unit

The insulation material of the hot-water tank unit of this water heater is reinforced. Figure 5 shows the appearances of both conventional insulation material and the reinforced insulation material. The conventional insulation material (Fig. 5(a)), glass wool, was wrapped around the stainless steel tank. With the new water heater, molded foamed polystyrene (PS) is configured to match the exterior shape of the tank to improve adhesion between the insulation material and the tank.

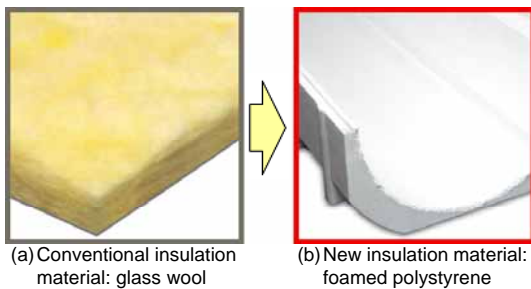


Fig. 5 Appearance of insulation material

As shown in Table 1, the thermal conductivity of the new heat insulation material is lower than that of the conventional material. In addition, the insulation structure is designed to increase the insulation of the connection pipe on the tank and controlled heat radiation by providing a gap between the insulation material and the housing covering the insulation material. As a result, the total heat insulation efficiency of the tank unit is improved such that the temperature inside the tank is reduced by approx. 15% over a certain period.

Table 1 Thermal conductivity of insulation material

	Glass wool for conventional specification	Foamed polystyrene for new specification
Thermal conductivity W/mK	0.038	0.034

## 5. Future Developments

With the HP water heater market rapidly expanding, the JIS for home-use HP water heaters will come into effect in April 2008. The details of the standard are currently being discussed.

The new JIS standard will change the evaluation reference from conventional “rating of COP (coefficient of performance)” to “actual operating efficiency of equipment” on annual basis, the same as for air-conditioners. This suggests key points for future technological development.

Since FY2006, manufacturers have been conducting joint studies with NEDO (New Energy and Industrial Technology Development Organization), and are likely to launch new products from next year based on the results.

We must continuously develop technologies to meet the changing performance evaluation criteria, improve the functionality of each system, expand the product range, and meet the need for energy saving measures.

## 6. Conclusions

Mitsubishi will strive to expand the sales of new products and continue to develop energy-saving plant facilities.

## 7. References

- (1) H. Maeyama et al.: Development of Rotary Compressor for CO<sub>2</sub> Heat Pump Water Heater, Mitsubishi Advance
- (2) H. Nakahide et al.: Technology for Controlling the Wear on the Top of Vanes Used for CO<sub>2</sub> Refrigerant Rotary Compressor, Mitsubishi Advance

# Rotary Compressor for a CO<sub>2</sub> Heat Pump Water Heater

Authors: *Hideaki Maeyama\** and *Shinichi Takahashi\**

## 1. Introduction

"ECO-CUTE" is a natural refrigerant heat pump water heater that uses CO<sub>2</sub>. The CO<sub>2</sub> refrigerant is highly efficient in water heating applications. However, because the operating pressure is very high and CO<sub>2</sub> has peculiar characteristics that are different from conventional refrigerants, we had to overcome some difficult technological challenges regarding the compressor used for this refrigerant. This report discusses these major technological challenges and the actual measures taken in the development of the Mitsubishi rotary compressor for CO<sub>2</sub> refrigerant.

## 2. Rotary Compressor

The rotary compressor mechanism consists of a rolling piston that rotates eccentrically in its cylinder and a vane installed in a vane slot in the cylinder that reciprocates along the slot causing the vane to move along the periphery of the rolling piston. As a result of the vane's movement, suction and compression chambers are formed inside the cylinder and the volume of each chamber changes in accordance with the rotation of the crankshaft to provide compression. Figure 1 shows a cross-sectional view of the Mitsubishi CO<sub>2</sub> compressor and Table 1 shows the major specifications thereof.

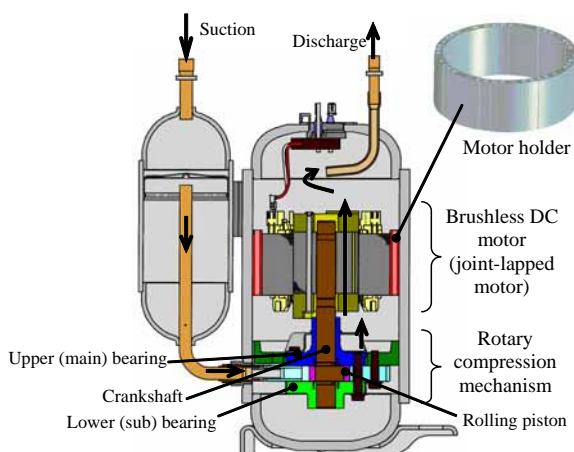


Fig. 1 CO<sub>2</sub> rotary compressor

Table 1 Specification of the CO<sub>2</sub> compressor

Compression system	Single rotary
Displacement	4.5 cm <sup>3</sup>
Refrigerant type	R744(CO <sub>2</sub> )
Motor	Brushless DC motor (joint-lapped motor)
Application	HP water heater

## 3. Characteristics of CO<sub>2</sub> Refrigerant

### 3.1 Environmental and safety characteristics <sup>(2)</sup>

- (1) CO<sub>2</sub> does not destroy the ozone layer. (Ozone depletion potential: ODP = 0.)<sup>1</sup>
- (2) CO<sub>2</sub> refrigerant has a low global warming potential. (Global warming potential: GWP = 1)<sup>2</sup>
- (3) CO<sub>2</sub> refrigerant is nonflammable.
- (4) CO<sub>2</sub> refrigerant has low toxicity.

### 3.2 Operating characteristics of CO<sub>2</sub> as a refrigerant

- (1) The operating pressure of CO<sub>2</sub> is high.
- (2) The speed of sound in CO<sub>2</sub> gas is very high.
- (3) The pressure of CO<sub>2</sub> rises to a high level in response to volumetric changes.
- (4) The density of the CO<sub>2</sub> refrigerant gas is high.

CO<sub>2</sub> refrigerant has excellent environmental and safety characteristics, as listed above. However, the use of CO<sub>2</sub> as a refrigerant involves some peculiar characteristics compared with conventional refrigerants.

## 4. Influence of CO<sub>2</sub> Refrigerant on a Compressor and Countermeasures

The influence of the characteristics of CO<sub>2</sub> mentioned above on a CO<sub>2</sub> compressor is taken into consideration as described below.

### 4.1 Pressure-resistant structure

The most remarkable characteristic of CO<sub>2</sub> refrigerant is that it has a high operating pressure. To cope with this, the compressor enclosure's pressure resistance requirements must be studied.

Figure 2 shows the operating pressure levels of the R410A Freon refrigerant used for room air-conditioners and similar equipment and that of natural CO<sub>2</sub> refrigerant used in the ECO-CUTE, together with the specifications of the enclosures for the respective refrigerants. As shown in Fig. 2, the operating pressure of CO<sub>2</sub>

refrigerant is approximately three times that of R410A, which requires the board thickness of the enclosure to be increased by more than double, proportionately.

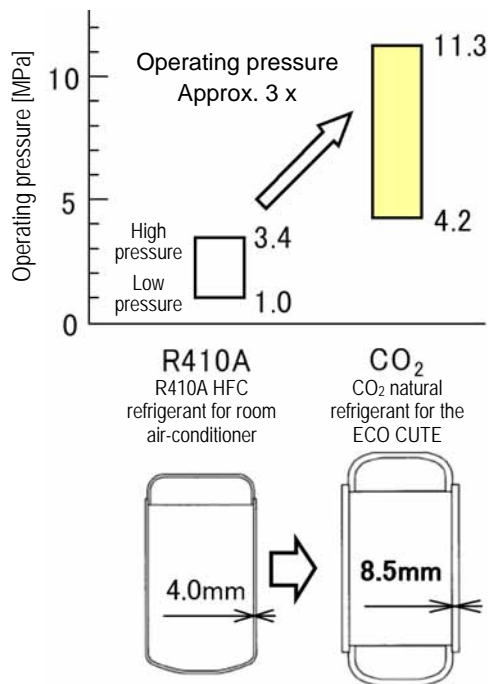


Fig. 2 Operating pressure of CO<sub>2</sub> and specification of the enclosure

#### 4.2 Securing efficiency

With a CO<sub>2</sub> refrigerant, which is characterized by high operating pressure, the speed of sound is very high and pressure rises quickly in response to volumetric changes. The amount of gas that passes through gaps between components in the rotary compression mechanism and leaks into the suction chamber from the compression chamber increases, making it difficult to attain appropriate efficiency in the same way as that applied to conventional refrigerant compressors. As a solution, we reduced the gap between the cylinder bore and the outer diameter of the rolling piston to narrow the gas leakage path. Moreover, we increased to the compression chamber in comparison to that in a R410A refrigerant compressor, to increase the sealing effect between components.<sup>(3)</sup> This countermeasure has increased the efficiency of the compressor. In addition, the COP (coefficient of performance) of the water heater system equipped with this compressor increased to one of the highest levels in the industry.

#### 4.3 Reduction in the oil circulation rate

One of the characteristics of the CO<sub>2</sub> refrigerant is that the gas has a high density. This particular characteristic affects the separability property of the refrigerant and the oil in the compressor's enclosure.

The gas, after being compressed by the rotary compression mechanism at the bottom of the compressor, is discharged into the space below the motor.

Thereafter, the gas passes through the motor into the upper space in the enclosure. Finally, the gas is discharged through the discharge pipe at the top of the compressor. The gas in the space below the motor contains a lot of oil, which is separated out as it passes through the motor. Because the density of the CO<sub>2</sub> refrigerant gas is about twice that of an R410A refrigerant, a large amount of oil is transferred into the space above the motor together with the refrigerant gas as it rises up through the motor. As a countermeasure against this phenomenon, we installed an additional motor-holder, as shown in Fig. 1. Because the motor-holder has a number of vertical holes, the gas passage area in the motor section is expanded to reduce the flow rate of the gas passing through the motor, thus reducing the amount of oil flowing into the space above the motor. As a result, an oil circulation rate of 0.1% was attained (at 60 rps).

#### 4.4 Achieving reliability of sliding portion

The high operating pressure of CO<sub>2</sub> refrigerant also seriously affects the reliability of the compressor's sliding portions. There are two types of sliding portions in the rotary compressor: one of them is the sliding portion around the crankshaft, which involves sliding of the main bearing, sub-bearing and rolling piston bore. Sliding is effected by the sliding bearing mechanism under thick-film lubrication conditions. Consequently, sliding durability can be secured under high operating pressure, if there are appropriate gaps in the bearing and oil of a suitable viscosity is used. The other sliding occurs around the vane, which is a part peculiar to rotary compressors. It is difficult to maintain thick-film lubrication conditions in this section: the section is easily subject to boundary or extreme-pressure lubrication conditions. It proved difficult to attain sliding durability in this section using the same method as that used in the R410A refrigerant compressor.

### 5. Achieving Reliability of the Sliding Portion around the Vane

This chapter focuses on achieving sliding durability of the sliding portion around the vane, which is one of the most important factors in realizing CO<sub>2</sub> rotary compressors.

#### 5.1 Configuration of the sliding portion around the vane

Figure 3 shows the configuration of the sliding portion around the vane in a rotary compressor and forces acting on the vane. There are two points around the vane where sliding conditions are harsh. One of these is between the side surface of the vane and the vane slot in the cylinder. Achieving sliding durability at this point is discussed in the following section. The other is

the sliding between the top of the vane and the periphery of the rolling piston. We coated the sliding part on the vane with a DLC-Si coating, which resulted in attaining sliding durability. This is one of the most difficult technologies applied in the development of the CO<sub>2</sub> compressor. A detailed explanation of this technology is provided in one of the other reports introduced in this issue; therefore, it will not be discussed in detail here.

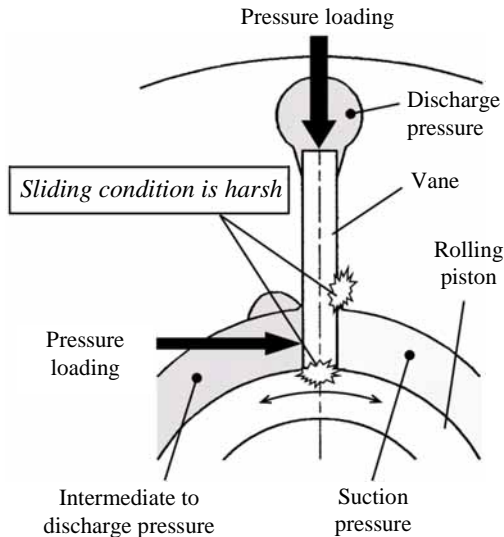


Fig. 3 Sliding portions around the vane

### 5.2 Achievement of sliding durability on the side surface of the vane

Figure 4(a) shows the detailed sliding conditions on the vane's side surface. The vane is inclined slightly due to pressure loading caused by the difference in pressures between the two sides of the vane: thereafter the side surface of the vane touches the corner of the vane slot bore in the cylinder. With the conventional R410A, the existing configuration gave sufficient sliding durability. However, the life test on this configuration,

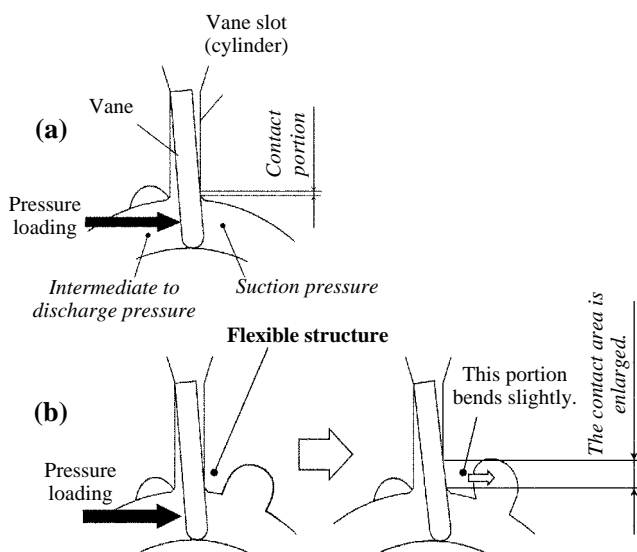


Fig. 4 Improvement in sliding condition of the vane's side

when using a CO<sub>2</sub> refrigerant, indicated faulty sliding within a short time.

To solve the problem, we installed a flexible structure in the vane slot in the cylinder, as shown in Fig. 4(b). This flexible structure is slightly bent when the side of the vane is loaded with pressure, thus expanding the contact area between the vane and the slot, which reduces contact pressure and eases the sliding condition.

There are two points that must be taken into consideration for the effective maintenance of this flexible structure. Firstly, the effect of reducing contact stress by expansion of the contact area as the flexible structure bends must be maintained. Secondly, the bend stress caused by the repetitive loading generated during the compressor's operation must be kept below the fatigue limit.

We then conducted a life test on the flexible structure, depending on several types of specifications. Figure 5 shows the bend stress of the flexible structure, the calculated value of the contact stress during contact with the vane, and the result of the life test with this particular specification.

The area where both the bend stress ratio and contact stress ratio of the flexible structure are below one, is the range in which the flexible structure is effective. We determined the specifications of the flexible structure based on the point indicated in the figure.

### 5. Conclusion

As described above, we improved the conventional R410A refrigerant compressor for the characteristics of the CO<sub>2</sub> refrigerant and successfully developed a new compressor with sufficiently high performance, oil circulation rate and reliability. The reliability of the vane sliding portions, in particular, was achieved by employ-

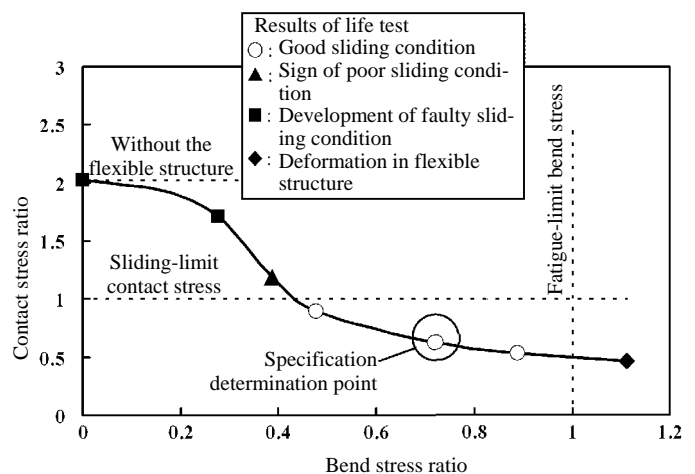


Fig. 5 Bend and contact stress at flexible structure

ing Mitsubishi's original technologies, such as the flexible structure for the cylinder vane slot and vane coating method (DLC-Si). As a result, we have successfully realized a compressor for a CO<sub>2</sub> refrigerant with a high operating pressure, namely the Single Rotary Compressor.

This compressor has been commercially supplied in Mitsubishi's ECO-CUTE range since autumn 2005 and has proved its top-of-the-industry performance and reliability in the market.

### References

- (1) T. Oikawa et al.: "Development of a High Efficiency Brushless DC Motor with a New Manufacturing Method of the Stator for Compressors," International Compressor Engineering Conference at Purdue (2002).
- (2) Edited by Heat Pump and Thermal Storage Technology Center of Japan under the general editorship of Hihara: "Non-freon Technologies: Trends in Natural Refrigerants", Ohmsha, Ltd., 2004.
- (3) T. Yokoyama et al.: Performance Analysis of CO<sub>2</sub> Refrigerant Rotary Compressor and Study for Improving the Efficiency, Annual conference of Japan Society of Refrigerating and Air Conditioning Engineers, 2005.
- (4) H. Maeyama et al.: "Development of a Compressor for CO<sub>2</sub> Heat Pump with a Single Rotary Mechanism," International Compressor Engineering Conference at Purdue (2006).

# Wear-Reducing Technologies for Rotary Compressors Using CO<sub>2</sub> Refrigerant

Authors: *Hideto Nakao\** and *Naotaka Hattori\*\**

## 1. Introduction

We employed a natural CO<sub>2</sub> refrigerant with a high operating pressure in a single rotary compressor. By coating the vane, for the first time in Mitsubishi rotary compressors, we intended to reduce the wear between the top of the vane and the outside of the rolling piston.

### 1. Application of a Coating to the Vane

Household heat pump water heaters not only use a natural CO<sub>2</sub> refrigerant, which has a high operating pressure, but also require a longer product lifetime than air-conditioning systems or refrigerating machines. In the early stages of development of the compressor, we used vanes prepared by nitriding high-speed steel in the same manner as conventional rotary compressors used for air-conditioning systems with the result that abnormal wear occurred at the top of the vane after operating for less than one-fifth of the lifetime needed. Then, we applied a DLC-Si to the vane, which is a coating of diamond-like-carbon containing silicon.

### 2. Characteristics of the DLC-Si

DLC-Si is accomplished with a plasma CVD (Chemical Vapor Deposition) method in which the coating forms in a plasma environment created by mixing a hydrocarbon gas and a gas containing silicon. With silicon contained in the film, the coating formed is thicker than general DLC, thus achieving better sliding and rolling characteristics.

Since the top of the vane of the rotary compressor and the outside of the rolling piston make line contact, the stress becomes severe and the contact involves both sliding and rolling phenomena.

When applying the coating to the vane, the adhesion strength between the coating film and the base material must be adequate, otherwise, the coating film may peel off and result in abnormal wear. It is necessary to identify the adhesion strength between the coating film and the base material for the appropriate application of the DLC-Si on the vane of a rotary compressor. We measured the adhesion strength with a micro scratch tester.

Figure 1 shows the relationship between the silicon concentration in the DLC-Si film and the adhesion strength between the coating film and the base material. According to Fig. 1, it is clear that the adhesion strength

between the DLC-Si film and the base material depends on the silicon concentration in the coating and is highest at a silicon concentration of approximately 20 wt%. It is also reported that the adhesion strength of the coating film depends on the internal stress developed at the interface and adhesion strength increases when internal stress is controlled properly.<sup>(3)</sup>

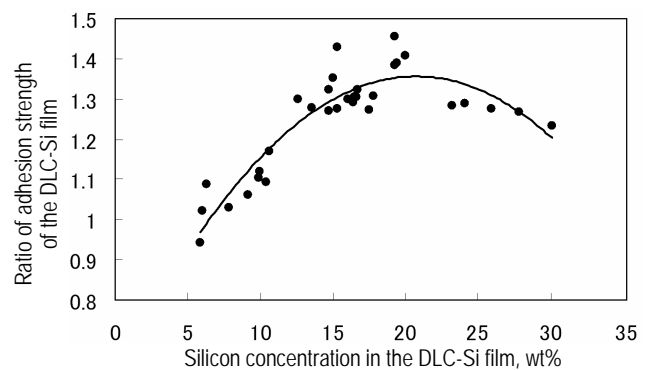


Fig. 1 The relationship between silicon concentration and the adhesion strength ratio of DLC-Si

In accordance with our examination results on the relationship between the silicon concentration in the film and the internal stress of the DLC-Si film applied to the vane of the rotary compressor, we confirmed that the lower the silicon concentration, the higher the internal stress, provided that the silicon concentration is 20 wt% or lower. This generally agrees with the reported characteristics mentioned above.

### 3. Structure of the Experimental Apparatus and Conditions of the Elemental Test

Table 1 shows the conditions of the wear test on the vane and rolling piston using the experimental apparatus.

Table 1 Conditions of elemental tests

Environment	CO <sub>2</sub>
Environment temperature	313K
Lubricant	PAG (VG-100: dropping)
Vane material	High-speed steel (nitriding treatment) High-speed steel (DLC-Si coated)
Rolling piston material	Special cast iron
Pressure loading	450N
Sliding velocity	0.6m/s

In this elemental test, a vane prepared by nitriding high-speed steel as well as a vane that conforms to treatment condition #5, shown in Table 2, were used.

**Table 2** The relationship between silicon concentration and adhesion strength of DLC-Si

Treatment conditions	Silicon concentration	Ratio of adhesion strength of the coating film
1	6wt%	1
2	13wt%	1.3
3	15wt%	1.35
4	17wt%	1.43
5	19wt%	1.46

On the other hand, in the life test (reliability evaluation test), using the rotary compressor as discussed in Chapter 4 below, we used a vane which was prepared by merely nitriding and vanes prepared with DLC-Si having five levels of adhesion strength, in accordance with treatment conditions #1 to #5. As shown in Fig. 1, the adhesion strength of the DLC-Si film changes with the silicon concentration in the film and especially with silicon concentrations between 5 and 20 wt%, the adhesion strength varies greatly with the silicon concentration. As a solution, we changed the hardness of the base material by changing the nitriding pretreatment conditions and the temperature of the plasma environment, as well as the supply of material gas during coating. As a result, the relationship between the silicon concentration in DLC-Si and the adhesion strength between DLC-Si and the base material was secured, as shown in Table 2.

**4. Conditions of the Life Test (Reliability Evaluation Test) Using a Rotary Compressor**

We conducted a life test on the rotary compressor, under the conditions shown in Table 3.

**Table 3** Conditions of reliability evaluation tests

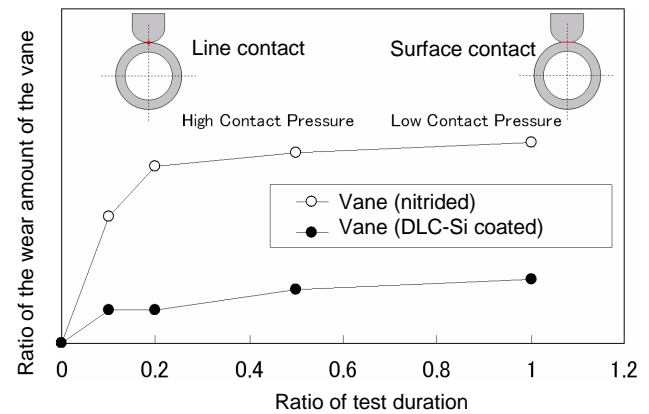
Refrigerant	CO <sub>2</sub>
Lubricant	PAG (VG-100)
Ps/Pd	3MPa/14MPa
Stoke volume	4.5cc
Vane material	High-speed steel (nitriding treatment) High-speed steel (DLC-Si coated)
Rolling piston material	Special cast iron

With the pressure inside the rotary compressor's shell at a higher level than the normal operating condition used for household heat pump water heaters and the rotational speed of the motor set at a higher level, which made the sliding conditions between the top of the vane and the periphery of the rolling piston more severe, we simulated an operating period equivalent to

the lifetime required for the product in a short period of time.

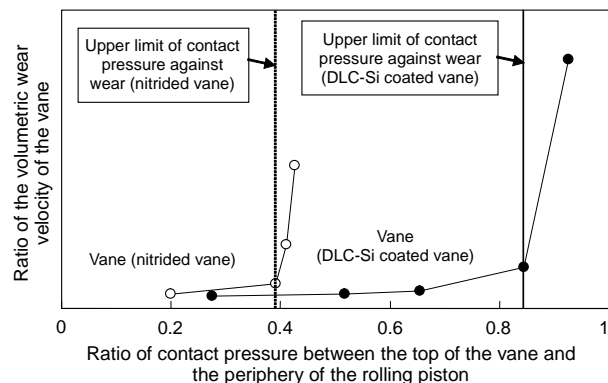
**5. Results of the Elemental Test and Considerations**

Figure 2 shows the ratio of the amounts of wear on the nitrided vane and the DLC-Si coated vane. The figure indicates, obviously, that the wear on the DLC-Si coated vane is much lower than that on the nitrided vane. This elemental test showed a tendency for wear on the vane to approach a certain level over time. This is attributed to a decrease in contact pressure due to the change from line contact to surface contact, which results from the increased wear on the top of the vane over a long period of testing time, as the vane slides in continuous contact with the rolling piston. Figure 3 shows the relationship between the contact ratio between the top of the vane and the periphery of the rolling piston, and the ratio of volumetric wear velocity.



**Fig. 2** Wear ratio of the vane in elemental wear tests

From Fig. 3, it becomes clear, with both the nitrided vane and DLC-Si-coated vane, that there is a flexion point where the volumetric wear velocity on the top of the vane increases sharply as the contact pressure between the top of the vane and the periphery of the rolling piston exceeds a certain value. The contact pressure between the top of the vane and the periphery of the rolling piston at the flexion point where the volu-



**Fig. 3** The relationship between the contact pressure ratio and wear velocity ratio of the vane

metric wear velocity increases sharply is the maximum contact pressure that controls the amount of wear on the vane. Based on the different flexion points shown in Fig. 3, the maximum contact pressure that controls the amount of wear on the DLC-Si coated vane is confirmed to be twice, or more, that of the nitrided vane.

### 6. Results of the Life Test and Considerations

Figure 4 shows the relationship between the ratio of test duration and the ratio of the amount of wear on the vane in the life test, using the nitrided vane and DLC-Si coated vanes with treatment conditions #1, #3, and #5 shown in Table 2.

For the test on the nitrided vane, the wear amount increased sharply and we suspended the test at the point where the ratio of operational length reached 0.2.

In the test on the DLC-Si coated vanes, the wear amount was most remarkably suppressed on the vane subjected to treatment condition #5, which had the highest coating film adhesion strength. The amount of

wear increased on the vane subjected to treatment condition #3, having lower adhesion strength than that of #5. However, these vanes developed slight wear only in the initial period of the operation, which appeared to be mild wear between the vane and the rolling piston. When the operating time was extended, the wear amount did not increase.

In the test on the vane subjected to treatment condition #1, in which the adhesion strength of the DLC-Si film was the lowest, we suspended the test at a test duration ratio of 0.1, when the DLC-Si film started to peel off.

Figure 5 shows the relationship between the ratio of the DLC-Si film's adhesion strength of the DLC-Si coated vanes subjected to treatment conditions #1 through 5, which were used in the compressor life test and the ratio of the amount wear on the vanes. Note that the values at the points where the operation reached durations that were equivalent to the lifetime needed for treatment conditions #2 through #5 and the value at a point where the DLC-Si film started to peel off for treatment condition

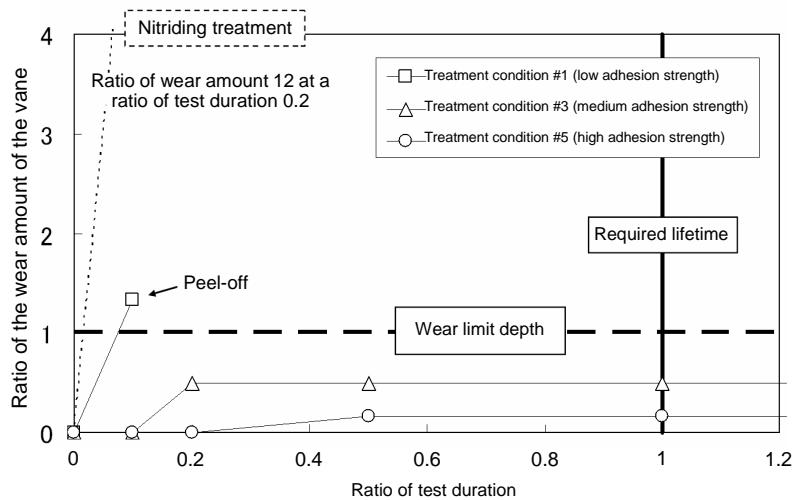


Fig. 4 The relationship between the test duration ratio and the wear volume ratio of the vane

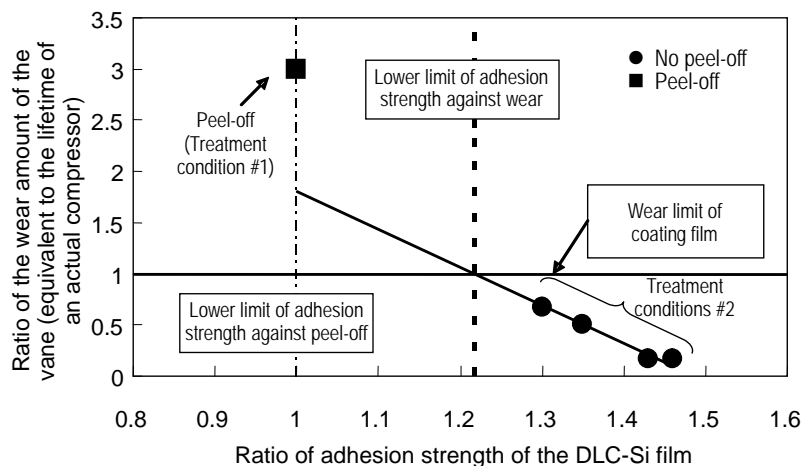


Fig. 5 The relationship between the adhesion strength ratio of DLC-Si and the wear volume ratio of the vane

#1, are indicated in the figure.

The approximate line of the test results of the vanes with treatment conditions #2 through 5 indicates that the amount of wear at the top of the vane increased with decreasing adhesion strength of the DLC-Si film. It also indicates that the film started to peel off when the ratio of adhesion strength was lowered to 1.

## **6. Conclusion**

By applying a DLC-Si to the vane, we developed a single rotary compressor that uses a CO<sub>2</sub> refrigerant for practical application in household heat pump water heaters for the first time in the world.

# Performance Analysis of Scroll Compressors Using CO<sub>2</sub> Refrigerant

Authors: *Mihoko Shimoji\** and *Toshiyuki Nakamura\*\**

## 1. Introduction

We manufactured a prototype of a large-capacity scroll compressor that uses CO<sub>2</sub> refrigerant, evaluated the performance of it, and analysed losses using a simplified model based on a basic test. As a result, the compressor input power levels in both the measurement and analysis agreed, although with a difference of approx. 3%, in the range of rotational speed from 30 to 100 rps. The availability of the analysis method was thus verified.

## 2. Specifications of the Prototype

For examination of the performance of a CO<sub>2</sub> compressor when used for air-conditioning (cooling), the authors manufactured a prototype compressor that uses CO<sub>2</sub> refrigerant, which is equivalent to 10HP and based on a mass-produced scroll compressor that uses R410A refrigerant.

The stroke volume of this compressor was designed to be approximately one-third ( $24 \times 10^{-6} \text{ m}^3/\text{rev}$ ) that of a R410A compressor, since the cooling capacity of CO<sub>2</sub> refrigerant per unit stroke volume is about three times that of the R410A refrigerant.

The operating pressure of CO<sub>2</sub> refrigerant is three times higher than that of R410A refrigerant and fluctuates with a large peak-to-bottom difference, resulting in a high operating load. For this reason, the reliability of the compressor was ensured by increasing the strength of the components such as compression part, and also by reinforcing the bearing support structure. In addition, for the prevention of refrigerant leakage, tip seals were applied to the axial leakage gaps in the scroll-wrap tips. Sliders<sup>(1)</sup> were used for sealing the leakage gaps in the radial direction on the scroll wrapside. (The turning radius of the orbiting scroll was changed during operation and this presses the orbiting scroll against the fixed scroll.)

## 3. Performance Evaluation of the Prototype

### 3.1 Evaluation conditions

Table 1 shows the evaluation conditions and stroke volume of the prototype. We evaluated the performance on the assumption that the prototype will be used for air-conditioning (cooling).

Table 1 Test conditions and stroke volume of the prototype

Item	Value
Suction pressure	4 MPa
Discharge pressure	10 MPa
Compression ratio	2.5
Suction temperature	15°C
Rotational speed	30rps/60rps/100rps
Stroke volume	$24 \times 10^{-6} \text{ m}^3/\text{rev}$

### 3.2 Results of the performance evaluation

Figure 2 shows the volumetric efficiency and overall adiabatic efficiency of the prototype under the operating conditions shown in Table 1. The efficiencies shown in Fig. 1 are the results of dividing the efficiency levels at each rotational speed by the efficiency level at 60 rps. The efficiency dropped significantly at low rotational speeds: the volumetric efficiency and overall adiabatic efficiency at 30 rps became lower than those at 60 rps by 17% and 16%, respectively.

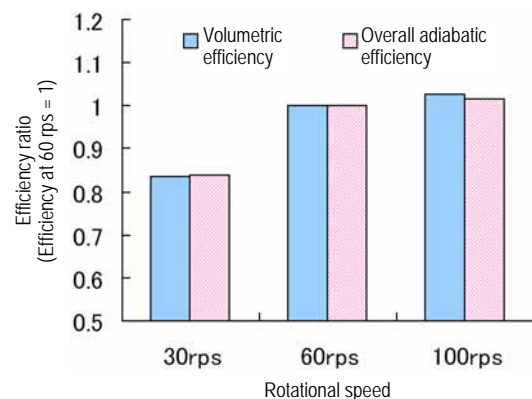


Fig. 1 Efficiency of the prototype

In the following chapters, we discuss loss analysis, using the methods described below to clearly identify the relationship between rotational speed and efficiency.

## 4. Loss Analysis

The input power to the scroll compressor is divided into theoretical compression power and various types of losses, as shown in Fig. 2. The respective types of losses are calculated based on pressure changes in the compression chamber. We are concerned here only with analysis methods of major losses.

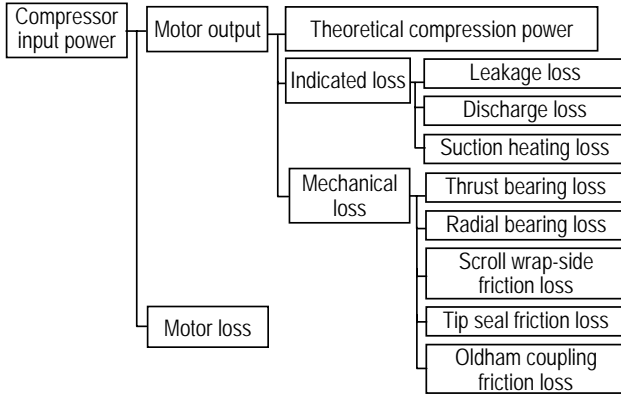


Fig. 2 Diagram of compressor input power

#### 4.1 Basic equations for the compression stroke

On the basis of the laws of conservation of mass and of conservation of energy and the changes in volume in the compression chamber, the changes in quantity of state in the compression chamber are expressed by equations (1) and (2) below.

$$dM = dM_{in} - dM_{out} \quad (1)$$

$$dU = \frac{1}{M} \{ (h_m - h) dM_m + P v \cdot dM - P \cdot dV \} \quad (2)$$

where,  $U$  = internal energy,  $M$  = mass,  $h$  = specific enthalpy,  $P$  = pressure in compression chamber,  $v$  = specific volume,  $V$  = volume of the compression chamber, suffix "in" indicates influx of refrigerant gas, and suffix "out" indicates outflow of refrigerant gas.

The basic equations in (1) and (2) above and changes in volume were used as simultaneous equations and the quantity of state in the compression chamber was determined by integration, for each compression chamber. Refprop7 is used as the refrigerant physical property program.<sup>(2)</sup>

#### 4.2 Leakage analysis model

The leakage flow rate  $\Delta G$  of  $\text{CO}_2$  refrigerant flowing through micro gaps is determined by multiplying the mass flow rate  $G_{ad}$  per unit area obtained by the equation of isentropic flow of the convergent nozzle by the leakage area  $S$  and leakage flow coefficient  $\alpha$ , which is described below.

$$\Delta G = \alpha S_c G_{ad} \quad (3)$$

The leakage gap in the axial direction of the scroll wrap tip and the leakage gap in the radial direction of the scroll wrap side were assumed to have been sealed with tip seals and the slider respectively. The refrigerant gas were assumed to leak only through the gap created at the side of the tip seal section. The dimensions of the gaps in the respective compression chambers were assumed to be the same taking account of thermal expansion and frame deformation under pressure during

operation.

The flow coefficient  $\alpha$  was determined in such a way that the left-hand side (leakage flow into the suction side calculated from measurement data) of the equation (4) was equal to the right-hand side (leakage flow into the suction side determined by calculation). The flow coefficient  $\alpha$  thus obtained was applied to all the leakage gaps.

$$\rho_{sh} V_{st} N - G_{exp} = \alpha \overline{S_c G_{ad}} \quad (4)$$

The first term on the left-hand side of equation (4) above is the amount of refrigerant circulating, determined by multiplying the density at a gas temperature measured immediately before suction into the compression chamber  $\rho_{sh}$ , by the stroke volume  $V_{st}$  and the rotational speed  $N$ . The second term on the left-hand side is the measured amount of refrigerant in circulation  $G_{exp}$ . The right-hand side indicates the leakage flow into the suction side, calculated periodically by equation (3) and averaged for a single rotation.

#### 4.3 Discharge model

When the pressure in the compression chamber becomes higher than the discharge pressure, as shown in Fig. 3, the discharge valve opens to release refrigerant gas.

Using the Bernoulli equation (5) below, the pressure rise  $\Delta P$  during discharge was determined on the assumption that the discharge is a permanent flow of incompressible fluid without friction.

$$\Delta P = \xi \frac{1}{2} \rho u_d^2 \quad (5)$$

In equation (5) above,  $\rho$  is the gas density in the compression chamber,  $\xi$  is the discharge loss coefficient, and  $u_d$  indicates the flow velocity at the opening area  $S_d$  at the discharge valve, shown in Fig. 3. It was also assumed that the valve lift would be at maximum during the gas outflow. The discharge loss coefficient  $\xi$  was set at 4.8 by taking into consideration the contraction of gas at the discharge port and also the inlet loss, bend loss and outlet loss.

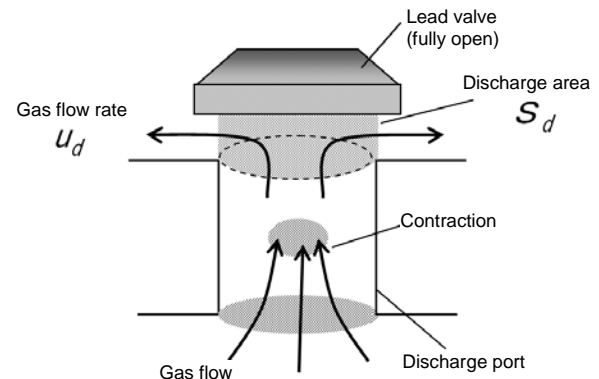


Fig. 3 Discharge model

#### 4.4 Thrust bearing loss model

The friction loss  $W_{TH}$  of the orbiting scroll and the thrust bearing is expressed by equation (6) below. In equation (6),  $F$  is the average gas load in the thrust direction, calculated from the pressure in the compression chamber,  $\mu$  is the friction factor,  $r$  is the orbital radius and  $N$  is the rotational speed. The value for the friction factor  $\mu$  above was determined by experiment, using the method of measuring the friction coefficient shown in Fig. 4, with lubricant dropped in a CO<sub>2</sub> refrigerant environment.

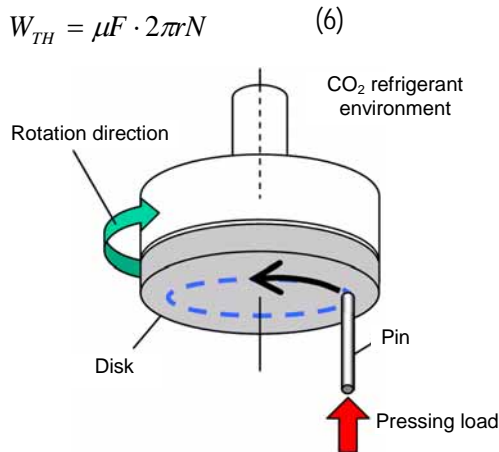


Fig. 4 Pin-on-disk type friction factor measuring equipment

#### 5. Results of Loss Analysis

Table 2 shows the prediction errors in the compressor input power values from analysis results under the evaluation conditions shown in Table 1. In Table 2, the prediction error in compressor input power is expressed by the equation  $\gamma = (\text{Analysis input} - \text{Measurement input}) / (\text{Measurement input}) \times 100[\%]$ .

Table 2 Prediction error of input power

Rotational speed	30 rps	60 rps	100 rps
Prediction error of input power: $\gamma$	+3.4	-3.0	-0.5

Table 2 indicates that the compressor input power levels in both the measurement and analysis agreed, albeit with a difference of approximately 3%, in the range of rotational speeds from 30 to 100 rps: the availability of the analysis method was thus verified.

Figure 5 shows the results of loss analysis for each rotational speed level.

Figure 5 indicates the values obtained by dividing each loss by the total loss. This figure shows that the rate of leakage loss is largest at 30 rps, which is approx. 2.7 times that at 60 rps. The rate of thrust bearing loss was the next largest. However, comparing the thrust load levels at respective rotational speed values revealed that the thrust load at 30 rps was more than 10% larger than those under conditions at 60 rps or higher. This could presumably be attributed to the fact that the pressure rise in the compression chamber due to leakage was larger than that at 60 rps. It means that thrust bearing loss can be reduced by improving the leakage conditions in the low rotational speed range. In addition, suction heating loss can be expected to decrease by reducing mechanical loss and increasing the amount of refrigerant circulating, thus improving the efficiency beyond the scale of leakage loss improvement.

Leakage loss was small at 100 rps, at which good performance was demonstrated, as shown in the figure.

Quantitative loss analysis of scroll compressors using CO<sub>2</sub> refrigerant was realized by using a simplified model based on a basic test. The authors will improve the performance of systems using this technology and also apply it to other compressors.

#### References

- (1) Fumiaki Sano et al., A High Reliability Study of the Scroll Compressor, Proceedings of the 1994 Purdue Compressor Conference (1994.7), pp. 199-204.
- (2) NIST, NIST Reference Fluid Thermodynamic Transport Properties – REFPROP Version 7.0 (2002.8).

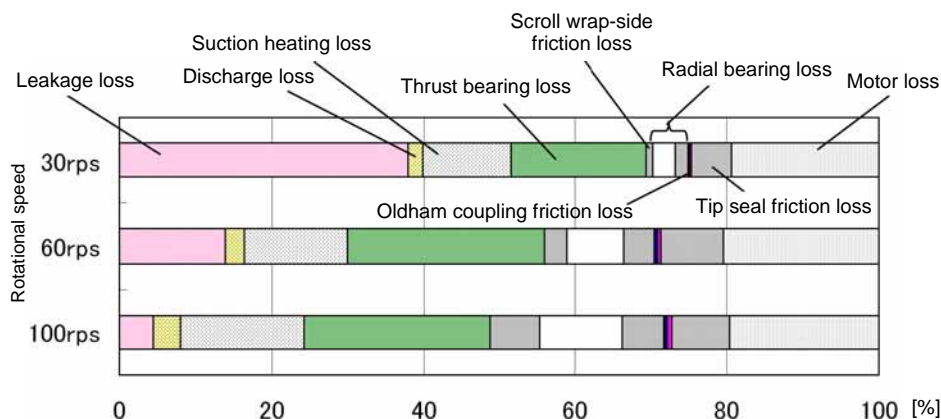


Fig. 5 Analysis of losses in the prototype

# Prototype and Performance Evaluation of Refrigerant-Refrigerant Microchannel Heat Exchanger

Authors: Susumu Yoshimura\* and Shinichi Wakamoto\*

## 1. Introduction

We developed a refrigerant-refrigerant microchannel heat exchanger, in which microchannel tubes consisting of several fluid paths through which low-temperature fluid and high-temperature fluid flow are joined, for the purpose of reducing the size and improving the performance of heat exchangers. From the results of performance evaluation of a prototype, we confirmed that the promotion of mixing of gas and liquid in the header could control the performance deterioration caused by maldistribution of a gas and liquid two-phase refrigerant, which was a major technological challenge in this type of heat exchanger.

## 2. Specifications of the Prototype and Test Method

### 2.1 Specifications of the Prototype

Figure 1 shows the prototype. Flat single tubes consisting of paths for the flow of low-temperature and high-temperature fluids, produced by aluminum extrusion, having a width of 25 mm and a thickness of 2 mm, are joined together. Two ends of the respective tubes are connected to the headers with a resultant configuration that provides five parallel flow units of low-temperature and high-temperature fluids. A single tube consists of 12 round microchannels having a cross-section with a 1 mm bore. The joints between singles tubes and between a single tube and the header are brazed together. The header bore is 6 mm and the effective length for heat exchange is 600 mm.

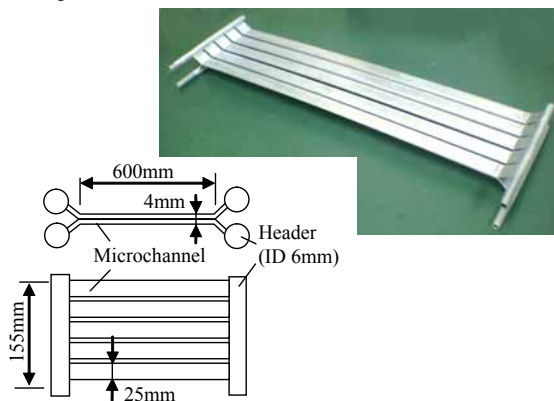


Fig. 1 Schematic view of the Prototype Heat Exchanger

### 2.2 Test conditions and test method

The operating fluids were R410A for cold fluid and water for hot fluid and these were counterflowed for heat exchange. Table 1 shows the test conditions. The cold fluid temperature  $T_{ci}$  and volume flow rate  $F$  of the hot fluid were fixed, while the hot fluid inlet temperature  $T_{hi}$ , mean mass velocity  $G$  of the cold fluid in the microchannel, and inlet quality  $X_i$  were changed. The header was positioned as shown in Fig. 2: (a) in a horizontal position and (b) in a vertical position. In a horizontal position, the heat exchanger was inclined at 50 degrees as shown in figure (a) and the fluid was introduced into the header horizontally and distributed downward vertically. On the other hand, in a vertical position, the fluid was introduced vertically and distributed horizontally. In the distribution section, the insertion  $\delta$  of a single tube into the header was set at 0 and 2 mm. The inlet length on the low-temperature side through which two-phase fluid flow was 200 mm. The thermal conductance of the heat exchanger  $AK$  was determined from the measured values of the inlet and outlet temperatures  $T_{ci}$  and  $T_{co}$  of the cold fluid, inlet and outlet temperatures  $T_{hi}$  and  $T_{ho}$  of the hot fluid, and volume flow rate  $F$ , using equation (1) below. The  $C_p$  and  $[LMTD]$  used in the equation are the specific heat at constant pressure and logarithmic mean temperature difference, respectively. The temperatures and flow rates mentioned below, unless otherwise specified, are those on the cold fluid side.

Table 1 Experimental conditions

$G$ kg/m <sup>2</sup> s	$F$ L/min	$T_{hi}$ °C	$T_{ci}$ °C	$X_i$ -
450 to 1300	2	37, 43	26.7	0.08 to 0.55

$$AK = \frac{\rho F C_p (T_{hi} - T_{ho})}{[LMTD]} \quad (1)$$

## 3. Results of the Test and Consideration

### 3.1 Single tube characteristics

First of all, to identify the characteristics without the influence of distribution, single tube characteristics were examined by removing one parallel flow unit from the

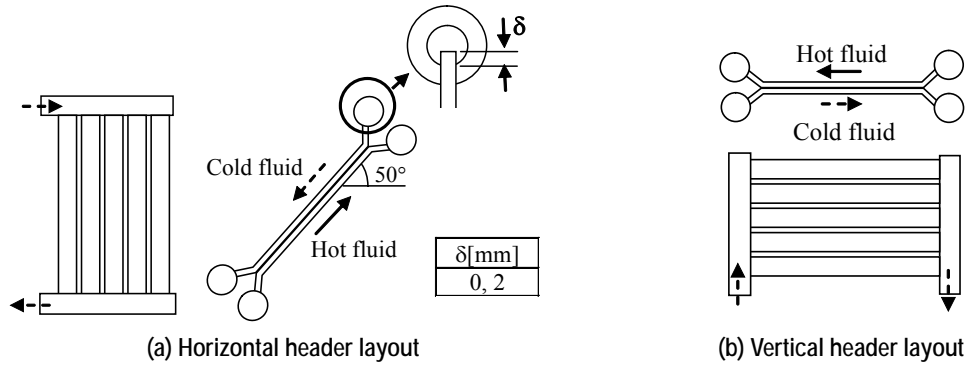


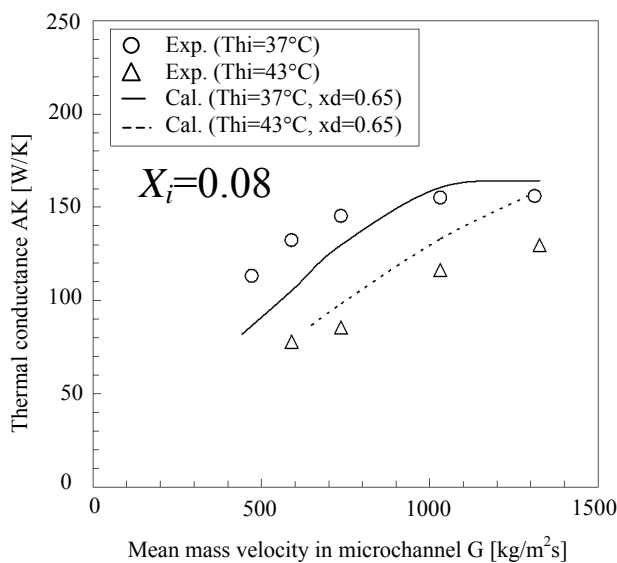
Fig. 2 Header layout and pipe insertion in the Prototype Heat Exchanger

prototype. The heat exchanger was set at an inclination of 50 degrees, as shown in the Fig. 2(a).

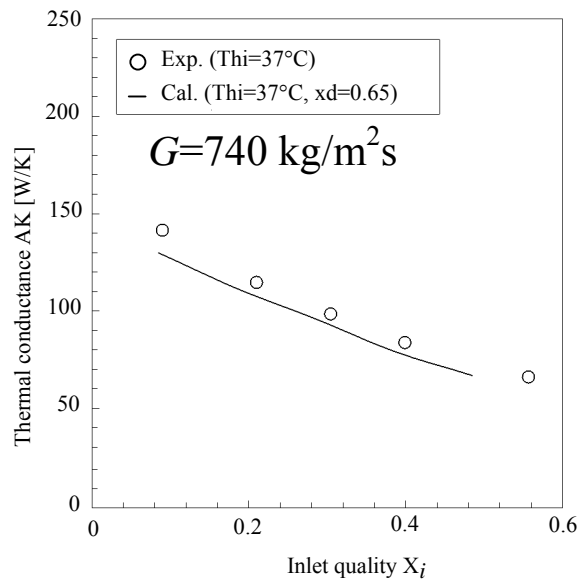
Figures 3(a) and 3(b) show the influence of the mean mass velocity  $G$  and inlet quality  $X_i$  in the microchannel on the thermal conductance  $AK$ , based on the results of the test. The marks  $\circ$  and  $\triangle$  in Fig. 3 indicate the hot fluid inlet temperature  $T_{hi} = 37^\circ\text{C}$  and  $43^\circ\text{C}$ .  $AK$  increased with the mass velocity  $G$  and decreased with increasing inlet quality  $X_i$ .  $AK$  also decreased with an increasing hot fluid inlet temperature  $T_{hi}$ .

Thereafter, we compared the test results with the results of the calculation, using the heat transfer calculation model described below. For the heat transfer model, the heat exchanger (length:  $L$ ) was divided into  $N$  elements in a longitudinal direction. Furthermore, as shown in Fig. 4, the heat exchanger was divided in the microchannel layout direction (number of channels:  $N_{ch}$  and pitch:  $p$ ). The value of  $N$  was 30. The thermal con-

ductance  $AK_i$  (microchannel wetted surface area basis) of each divided element "i" consisted of heat transfer coefficients (heat transfer coefficients  $\alpha_h$  and  $\alpha_c$ ) of the hot and cold fluids, thermal conductivity of the flat tube (thermal conductivity of material  $\lambda_t$ ), and thermal contact conductance  $\alpha_{cl}$  of the brazing layer.  $L_i$  is the length of an element. For thermal conduction of the flat tube, it was divided into the portion contacting the brazing-layer (portion A) and the portion between the centers of channel holes (portion B). Portion B was expressed by a fin having a wetted perimeter  $\pi D$ , an average thickness  $t_{av}$ , length  $D$ , thermal conductivity  $\lambda_t$  and efficiency  $\phi$ . The applicability of the fin mentioned above to represent portion B reasonably was verified previously by a two-dimensional numerical calculation. "t" is the distance from the brazing layer to the microchannel. Dittus-Boelter's equation<sup>(1)</sup> was used for the heat transfer coefficient  $\alpha_h$  of the hot fluid, while Yu et al.'s equation<sup>(2)</sup> was used for the heat transfer coefficient  $\alpha_c$  of the cold two-phase fluid. Furthermore, the dryout zone taken into the heat transfer coefficient  $\alpha_c$



(a) Relation between  $G$  and  $AK$



(b) Relation between  $X_i$  and  $AK$

Fig. 3 Thermal conductance with varying mean mass velocity and quality in the microchannel

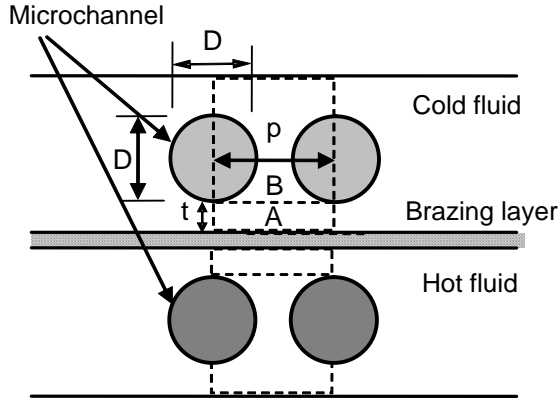


Fig. 4 Schematic view of the hat transfer model

was calculated by Dittus-Boelter's equation on the assumption that the heat transfer coefficient is that in gas single-phase flow at dryout quality  $X_d$  or higher. For the value of  $X_d$ , the average 0.65 of the values, 0.6 to 0.7, reported in the study on the characteristics of evaporating heat transfer of microchannel tubes by Kuwahara et al.<sup>(2)</sup> was used.

Calculations for AK are expressed by equations (2) through (5) below. The thermal contact conductance  $\alpha_{cl}$  was obtained by first performing an experiment on water-to-water heat exchange, and next by determining the value of AK from equation (1), and then calculating equations (2) to (5), to finally obtain  $\alpha_{cl} = 1.7 \times 10^5$  W/m<sup>2</sup>K. Since both the cold and hot fluids are a single-phase flow in this case,  $\alpha_c$  was also determined by Dittus-Boelter's equation. The value of AK was thus calculated by using equation (2) from the heat transfer rate Q, which was the total sum of the heat transfer rate of the respective divided elements.

$$Q = AK[LMTD] = \sum_i^N AK_i[LMTD]_i \quad (2)$$

$$AK_i = \pi DN_{ch} L_i \left\{ \frac{1}{\phi_h \alpha_h} + \frac{2\pi D}{p} \frac{t}{\lambda_t} + \frac{\pi D}{p \alpha_{cl}} + \frac{1}{\phi_c \alpha_c} \right\}^{-1} \quad (3)$$

$$\phi = \frac{\tanh \left( \frac{(\pi D) \alpha}{\lambda_t t_{av}} \right)}{\sqrt{\frac{(\pi D) \alpha}{\lambda_t t_{av}}}} \quad (4)$$

$$t_{av} = p - \frac{\pi}{4} D \quad (5)$$

Figure 3 shows the results of the calculations: the solid line for  $T_{hi} = 37^\circ\text{C}$  and the dotted line for  $T_{hi} = 43^\circ\text{C}$ .  $T_{hi} = 37^\circ\text{C}$  and  $T_{hi} = 43^\circ\text{C}$  correspond to the average heat flux of approximately 40 kW/m<sup>2</sup> and 50 kW/m<sup>2</sup>. The trends in the calculated and experiment values largely agree. On the other hand, the difference between the calculated values and experiment values

could be attributed to the dryout quality  $X_d$  and the heat transfer models in the dryout zone.

### 3.2 Performance of the prototype

Figure 5(a) shows the relationship between the thermal conductance AK of the prototype and the mass velocity  $G_{hd}$  at the inlet header (horizontal axis), while Fig. 5(b) shows the relationship between the thermal conductance AK of the prototype and the inlet quality  $X_i$  (horizontal axis). The  $\circ$  marks in the figure indicate values that are five times the AK and  $G_{hd}$ , obtained on the basis of the single tube characteristics described in section 3.1 above. The AK of the prototype grew to be AK = 480 through 700 W/K at  $X_i = 0.08$  and  $G_{hd} = 800$  to 1200 kg/m<sup>2</sup>s in the horizontal position and a pipe insertion at distribution section of  $\delta = 2$  mm (marked with  $\bullet$  in the figure) and decreased to AK = 700 to 490 W/K for  $X_i = 0.08$  to 0.3. The mean mass velocity G in the microchannel was G = 450 to 700 kg/m<sup>2</sup>s in the range of  $G_{hd} = 800$  to 1200.

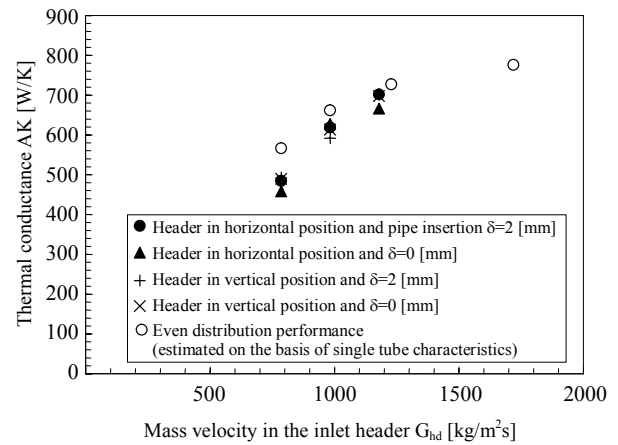
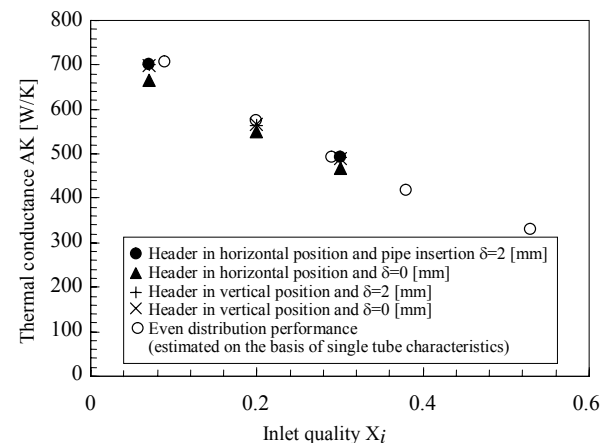

 (a) Relation between  $G$  and AK

 (b) Relation between  $X_i$  and AK

Fig. 5 Thermal conductance with varying mean mass velocity and quality in the microchannel

Compared with the single tube characteristics, performance deterioration assumed to be attributable to maldistribution was found to be 2 to 5% for  $G_{hd} = 1000$

or higher, which was shown to be comparatively small. Regarding inlet quality  $X_i$ , the larger  $X_i$  was, the more the performance deterioration was reduced. The influence of the header position or the pipe insertion at the distribution section on performance, was confirmed to be limited.

The factor of the findings mentioned above can be explained as follows.

In Fig. 6, the horizontal axis shows the corrected gas mass velocity, calculated by dividing the mass velocity  $G_g$  of the refrigerant gas in the inlet header as expressed by equation (6) by parameter  $\lambda^{(3)}$  in the Baker map, which is used as the flow regime map of the two-phase flow, while the vertical axis shows the ratio of the thermal conductance  $AK$  to  $AK$  during even distribution without maldistribution. (The value was obtained by dividing the data marked with ●, ▲, +, and × by the data marked with ○ in Fig. 5.)

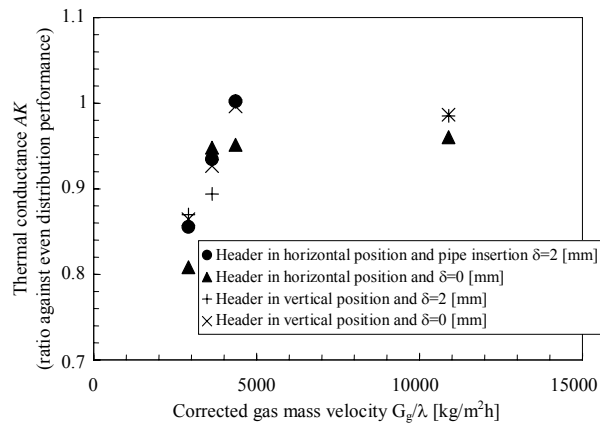


Fig. 6 Thermal conductance with varying corrected mass velocity in the header

$$G_g/\lambda = X_i G_{hd}/\lambda \quad (6)$$

$AK$  increases with increasing  $G_g/\lambda$  to gradually approached 1. From this, it can be assumed that the reason why even distribution is advanced with increasing flow rate and inlet quality, and performance deterioration is consequently reduced, is that the gas velocity increases in the inlet header and the mixing of gas and liquid is increased in the flow.

The authors clearly identified the basic characteristics of the refrigerant-refrigerant microchannel heat exchanger. The authors are going to expand the range of conditions for evaluating the characteristics and continue the study to improve flow distribution.

### References

- (1) F. W. Dittus, L.M.K. Boelter: Univ. Calif. Publ. Eng., 2, 433 (1930).
- (2) K. Kuwahara et al.: Trans. of JAR, 21(2), 121-128 (2004).
- (3) O. Baker: J. Oil & Gas, 53, 185 (1954).

